THE ASTROPHYSICAL JOURNAL, 237:529–540, 1980 April 15

EVOLUTION OF BALMER-LINE EMISSION PROFILES OF V1500 CYGNI IN THE EARLY DECLINE PHASE[1]

A. SANYAL
Iowa State University and University of Shiraz, Iran
AND
L. A. WILLSON
Iowa State University
Received 1978 October 30; accepted 1979 October 18

ABSTRACT

The emission lines of the hydrogen Balmer series, during much of the early decline phase, consist of four major components whose relative intensities evolve with time. The evolution of the major components of the lines with time is examined in this paper in terms of a simple parametrization scheme involving four identical condensations which radiate anisotropically. The simple parametrization describes the evolution of the major components quite well, and leads to the conclusion that the anisotropy of the radiation from the condensations is the most important parameter, and that geometrical parameters (such as the inclination of the system and the condensation size relative to the system size) are probably relatively model independent. The anisotropic radiation from each condensation is suggested to be a consequence of their being partially ionized; a theoretical anisotropy factor as a function of time based on that assumption proves very satisfactory. This in turn leads to order-of-magnitude estimates for the ultraviolet flux of the ionizing source and mass of the ejecta: $S_{UV} \approx 10^{48}$ photons s^{-1} and $M \approx 4 \times 10^{-5} M_{\odot}$.

Subject headings: stars: individual — stars: novae

I. INTRODUCTION

V1500 Cygni was one of the most spectacular novae of the present century and has been extensively observed and discussed: see for example *Astronomischeskii Zhurnal*, Vol. **54** (1977; issue on Nova Cygni), Ennis *et al.* (1977), Ferland (1977), Ferland, Lambert, and Woodman (1977), Gallagher and Ney (1976), Jenkins *et al.* (1977), Sanyal (1976), and Strittmatter *et al.* (1977).

In this paper we discuss the evolution of the Balmer emission line profiles in the early decline phase of Nova Cygni 1975 based on measurements of high-dispersion spectra obtained at the Dominion Astrophysical Observatory. Our goal is to present an analysis of the emission line profiles using as simple a parametrization scheme as is consistent with both the data and our present understanding of the nature of novae. With this scheme we seek to isolate geometrical factors—size and inclination angles—from physical variables such as source function or ionization state. Our results suggest that changes in the physical variables are very important in the evolution of the line profiles, at least during the early decline phase.

[1] Biruni contribution No. 6.

II. OBSERVATIONAL BASIS

The observations used in our analysis were obtained at the Dominion Astrophysical Observatory, Victoria, Canada, by the observatory staff with the coudé focus of the 1.2 m telescope. The spectra were obtained using IIa-O emulsion for the blue plates and IIa-F for the red, using standard techniques. The dispersion varied from 6.5 Å mm^{-1} to 17.9 Å mm^{-1} at Hγ. The spectra were converted into relative intensity tracings using the COSMOS machine at the observatory. The radial velocities were obtained from the tracings using a procedure described by Sanyal (1976).

Sample Hβ intensity profiles for observations taken between 1975 September 3 (JD 2,442,659) and October 2 (JD 2,442,688) are shown in Figure 1. The dominant structure consists of four main components which, in time, split into many (as had been noted for other novae). We have chosen to label the main components *a–d*, progressing from blue to red. In Table 1 we have listed the ratios of the intensities of the main component to the extreme blueshifted component *a*. Observational uncertainties should be less than $\sim 5\%$ in these ratios. We have also tacitly assumed that there is no differential reddening across the profile; intranebular reddening $\propto 1/\lambda$ such as found by Hutchings and Fisher (1973) for nova FH Ser would introduce

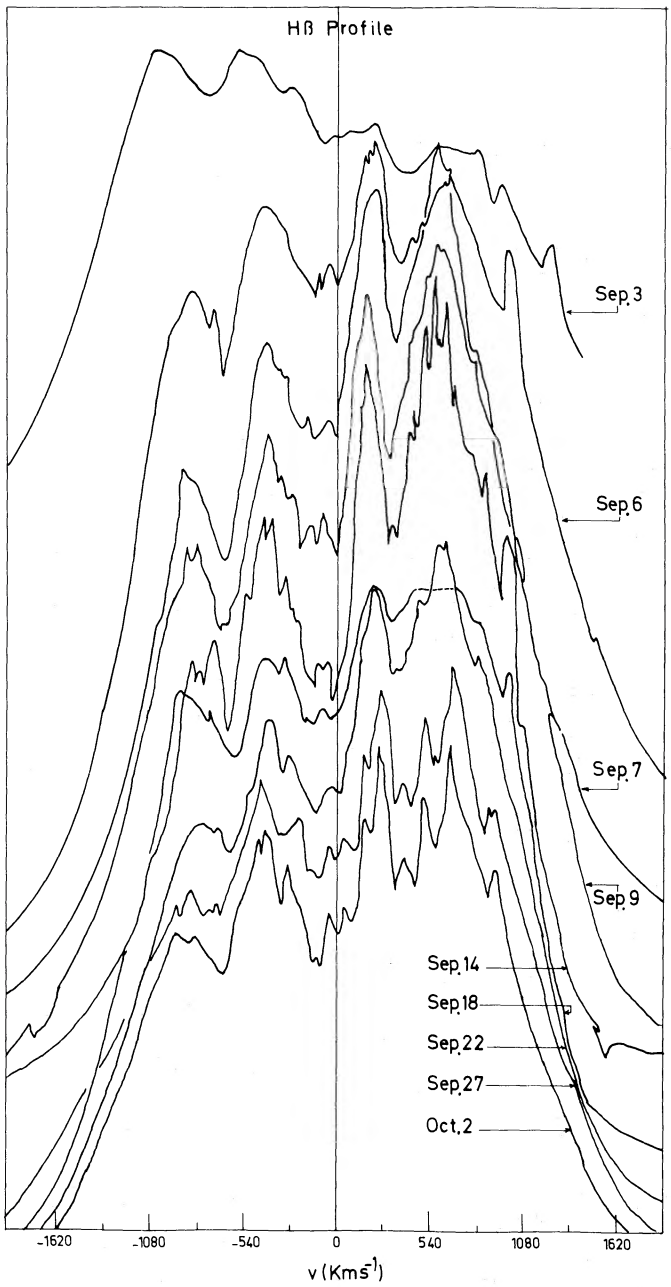

FIG. 1.—Relative intensity tracings of Hβ emission line profiles for Nova Cygni 1975 for nine dates between 1975 September 3 and October 2 from high-dispersion spectra obtained at the Dominion Astrophysical Observatory. Spectra for different dates have been shifted by an arbitrary amount with respect to the vertical (intensity) axis.

additional errors of $\sim 10\%$ in these ratios and would have the effect of increasing the anisotropy parameter values (see § IV) by a comparable amount. The major trend in the evolution of the line profiles is evident from Figure 1 and Table 1: the redshifted components are initially weaker than the blueshifted ones, but they become stronger within a few days of the outburst, reach maximum relative intensity after roughly two weeks, and then slowly evolve towards equal intensities. It is this variation of the relative intensities of the components of the emission lines with time which forms the observational basis for this paper.

III. THE PARAMETRIZATION SCHEME

In order to explain as simply as possible the evolution of the four principal components of the emission lines, we shall assume a simple "model" consisting of four condensations of matter ejected

TABLE I

RELATIVE INTENSITIES OF THE PRINCIPAL COMPONENTS OF THE HYDROGEN LINES[a]

DATE (1975)	Hα			Hβ			Hγ			Hδ		
	b/a	*c/a*	*d/a*	*b/a*	*c/a*	*d/a*	*b/a*	*c/a*	*d/a*	*b/a*	*c/a*	*d/a*
Sept. 2	1.06	0.86	0.75	...	...	...	...	...	...	...	...	...
Sept. 3	...	...	...	1.0	0.85	0.81	1.02	0.96	0.93	1.04	1.08	1.11
Sept. 4	1.08	0.97	0.95	...	...	...	...	...	...	...	...	...
Sept. 5	1.10	1.12	1.05	...	...	...	...	...	...	...	...	...
Sept. 6	...	...	...	1.14	1.24	1.08	1.16	1.30	1.13	1.17	1.37	1.33[b]
Sept. 7	1.19	1.37	1.41	...	...	...	1.24	1.55	1.63	1.13	1.50	1.60[b]
Sept. 9	...	...	...	1.18	1.40	1.48	1.31	1.57	1.67	1.09	1.40	1.51[b]
Sept. 10	...	...	...	...	...	...	...	...	...	1.07	1.30	1.34[b]
Sept. 14	...	...	...	1.27	1.62	1.78	1.34	1.59	1.75	1.10	1.28	1.41[b]
Sept. 18	1.03	1.44	1.51	1.30	1.83	2.02	...	...	...	1.14	1.41	1.35[b]
Sept. 22	...	...	...	...	...	...	1.21	1.48	1.55	1.03	1.20	1.18[b]
Sept. 27	...	...	...	...	...	...	1.34	1.75	1.90[b]	1.04	1.12	1.09[b]
Sept. 28	...	...	...	1.34	1.64	1.70	...	...	...	...	...	...
Oct. 1	...	...	...	1.26	1.51	1.49	...	...	...	...	...	...
Oct. 2	...	...	...	...	...	...	1.24	1.64	1.81[b]	1.00	1.09	1.09[b]

[a] Probable errors on relative intensities are ~5% (see Hutchings *et al.* 1978).
[b] Possible blending affecting one or more components.

from the nova, with each condensation corresponding to a single component of the emission lines. For simplicity we assume the blobs are identical. To conserve momentum, they must emerge in pairs; the final simplification comes from assuming that the pairs emerge with equal velocities and in a pair of directions at right angles to one another (see Fig. 2).

In order to account for the different brightnesses of the components, we will invoke two independent effects: occultation of one blob by another one and anisotropy of the radiation emerging from each blob. Only when we seek to interpret the occultation effects quantitatively or to interpret the anisotropy in terms of a detailed physical model does the geometry of the blobs become important; at that point a more rigorous model should include a consideration of the optical depth of the blobs as well. A simplified calculation of the occultation to be expected for opaque, spherical blobs is presented in § IV*c*; for the rest of the geometric analysis the assumption of identical blobs of arbitrary shape is sufficient.

The schematic model which forms the basis for the parametrization scheme is sketched in Figure 2. We assume that four identical condensations (blobs) give rise to the four major components of the emission lines; these four blobs are labeled *a–d* in Figure 2 to correspond to the emission components *a–d* defined in § II. The coordinate system in which most of the equations will be expressed has the line of sight as the *x*-axis, which is positive towards the observer. The initial coordinate system, which is related to the final one by two successive rotations, has the line *ad* as the *x*-axis, reckoned positive in the direction from *d* to *a*. In

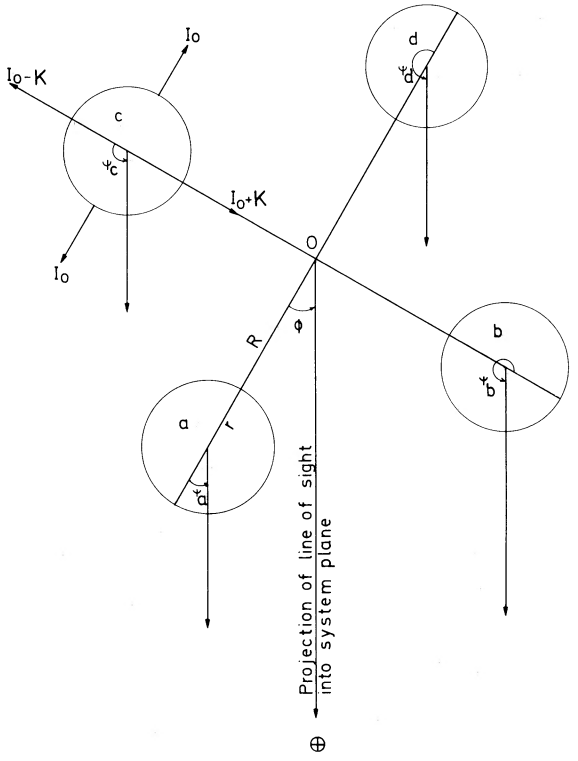

FIG. 2.—The geometry underlying the parametrization scheme is shown in this figure representing the four-blob schematic model. The angle ϕ is the angle between the line *ad* and the projection of the line of sight into the plane of the system. The system plane is assumed to be inclined by an angle *j* with respect to the plane of the sky.

the initial coordinate system the positions and velocities of the blobs are very simple to express: for example, $\boldsymbol{R}_a$(initial) = (R, O, O) and $\boldsymbol{v}_a = (dR/dt, O, O)$. Performing two successive rotations on this coordinate system—first, a rotation by ϕ about the z-axis and then a rotation by $(\pi/2 - j)$ about the (new) y-axis—we arrive at an expression for the positions of the centers of the condensations:

$$\boldsymbol{R}_a = -\boldsymbol{R}_d = (R\cos\phi\sin j, -R\sin\phi, R\cos\phi\cos j),$$
$$\boldsymbol{R}_b = -\boldsymbol{R}_c = (R\sin\phi\sin j, R\cos\phi, R\sin\phi\cos j). \quad (1)$$

For each blob the emitted intensity is assumed to vary when viewed from different angles, with the brightest part that facing the center of the system. We assume for simplicity that the variation is given by

$$I_i/I_0 = 1 + K\cos\Psi_i, \quad (2)$$

where I_0 is the mean brightness (assumed equal for our four identical blobs), K is a constant between 0 and 1, and Ψ_i is the angle between the line of sight, $\hat{x}$, and $\boldsymbol{R}_i$. The intensity radiated towards the system center is thus $I = I_0(1 + K)$; directly away from system center the intensity radiated is $I = I_0(1 - K)$, and at 90° it is just $I = I_0$. Note that since the system is inclined by an angle $(90° - j)$ with respect to the line of sight, the angle Ψ is not measured in the system plane unless $j = 90°$. When $j = 90°$ we find simple expressions for Ψ_i in terms of ϕ as sketched in Figure 2: $\Psi_a = \phi$, $\Psi_b = (\pi/2) - \phi$, $\Psi_c = (\pi/2) + \phi$, and $\Psi_d = \pi - \phi$.

For the more general case, $j \neq 0$, and for observations taken when there is no occultation of the blobs by each other, equations (1) and (2) plus inspection of Figure 2 yield directly the normalized intensities of the four components:

$$I_a/I_0 = 1 - K\cos\Psi_a \equiv 1 - K\cos\phi\sin j,$$
$$I_b/I_0 = 1 - K\cos\Psi_b \equiv 1 - K\sin\phi\sin j,$$
$$I_c/I_0 = 1 - K\cos\Psi_c \equiv 1 + K\sin\phi\sin j,$$
$$I_d/I_0 = 1 - K\cos\Psi_d \equiv 1 + K\cos\phi\sin j. \quad (3)$$

Before September 6 (JD 2,442,662) the intensities of the redshifted components are lower than those of the blue shifted components, i.e., equation (3) cannot account for the relative intensities. We assume that this is due to occultation of the farther, receding condensations by the closer ones. From Figure 2 it is apparent that in practice only two types of occultation are possible: a blocks c and b blocks d by an amount q_1; a blocks d by an amount q_2. Thus we can generalize equation (3) to include occultation to give:

$$I_a/I_0 = 1 - K\cos\phi\sin i,$$
$$I_b/I_0 = 1 - K\sin\phi\sin i,$$
$$I_c/I_0 = (1 + K\sin\phi\sin i)(1 - q_1),$$
$$I_d/I_0 = (1 + K\cos\phi\sin i)(1 - q_1 - q_2). \quad (4)$$

Here we have made no assumptions regarding the geometry of the individual blobs, and thus the occultation parameters q_1 and q_2 are independent free parameters to be fitted by the observations. For the special case of spherical blobs the parameters q_1 and q_2 are of course completely determined once we know ϕ, j, and R/r.

From our definitions we can write the line-of-sight velocities of the condensations as

$$v_a = -v\cos\phi\sin j = \frac{d\boldsymbol{R}_a}{dt}(\hat{x}),$$
$$v_b = -v\sin\phi\sin j,$$
$$v_c = +v\sin\phi\sin j,$$
$$v_d = +v\cos\phi\sin j, \quad (5)$$

where $\hat{x}$ is the unit vector in the direction of the observer, and astronomical convention is used for the signs of the velocities. We will be using equation (5) to determine $\tan\phi = v_b/v_a = v_c/v_d$ from the observed velocities.

How many parameters are there in this model which need to be determined from the observed velocities and the relative intensities of the four major components? For the case of spherical blobs there are two parameters with the dimensions of length: R = the distance of the center of each blob from the center of the system, and r = the blob radius. The two angles needed to describe the orientation of the system are j = the inclination of the system to the plane of the sky, and ϕ = the angle of rotation of the x-axis with respect to the projection of the line of sight into the plane of the system. The velocity parameters are $w = dr/dt$ and $v = dR/dt$. Finally, we have the anisotropy parameter K, for a total of seven parameters. In practice, however, the free parameters required to fit the data are fewer than seven: the amount of blocking depends only on the ratio R/r, not on r and R individually; also, since $w \ll v$ (§ IV), we may, for purposes of deriving the geometry, neglect one of the velocity parameters; finally, $\sin j$ may be combined in many cases with other parameters, so that we determine, for example, the single parameter $(K\sin j)$ rather than both K and j. The observed quantities are three intensity ratios (I_b/I_a, I_c/I_a, and I_d/I_a), a velocity ratio $v_b/v_a = v_c/v_d$, and the absolute velocities $v\sin j$ (from the reduction of v_i using $\tan\phi = v_b/v_a$) and w (from the width of the individual components) for a total of six numbers. Thus, in principle, we can completely determine the parameters describing the system of four spherical condensations. If, on the other hand, we do not assume spherical blobs, then we cannot derive from this set of observational quantities any information on the angle j nor any rigorous information on our measure of the size of the individual blobs, r, or their separation R. In that case q_1 and q_2 are independent, and our free parameters reduce to these six: ϕ, $K\sin j$, q_1, q_2, $v\sin j$, and w. In either case, for spherical or for arbitrary

condensations, the six observed quantities are sufficient for a unique set of derived parameters to be specified.

In § IV we shall use equations (4) and (5) to derive from the data the parameters ϕ, $(K \sin j)$, q_1, and q_2 for the hydrogen Balmer lines for dates between 1975 September 3 (JD 2,442,659) and 1975 October 2 (JD 2,442,688). Since these parameters are completely determined by the velocities and intensities of the components of one line at one instant, a comparison of the results for different lines on a given date and of the results for different dates give internal consistency checks on the applicability of the model.

IV. DERIVATION OF THE PARAMETERS FROM THE OBSERVATIONS

The derivation of the parameter values from the observed velocities and intensities is straightforward. First, the velocities are used to find ϕ. Next the intensities of the components can be plotted as a function of $\cos \phi / \sin j$. An attempt is then made to fit all four intensities using equation (3). If that succeeds, we can derive from that fit a value for $(K \sin j)$. Equation (3) holds when occultation effects are absent, that is, when the blobs are sufficiently far apart that they do not block each other. Thus, when we can fit the relative intensities using equation (3), we find $(K \sin j)$ well determined, but we can only at best derive a lower limit on R/r. If, on the other hand, equation (3) does not fit the relative intensities, then we use equation (4). In that case we find $(K \sin j)$, q_1, and q_2 from fitting the three, independent, relative intensities. That is, if we cannot fit all four intensities with a single $(K \sin j)$, we proceed to fit I_a and I_b (or I_a, I_b, and I_c) only. According to this model (eq. [4]), I_c and I_d can only lie below the intensities predicted by equation (3) and I_a, I_b. From $(K \sin j)$ and I_c/I_a we derive q_1; from $(K \sin j)$, I_d/I_a, and q_1 we derive q_2. Note that q_2 depends on the other parameters and is thus the most sensitive to errors in data, analysis, and assumptions: $(K \sin j)$ depends only on the accuracy with which ϕ can be determined and uncertainties in I_b/I_a and is, thus, relatively well determined.

a) Derivation of ϕ from the Observed Velocities of the Components

In this section we shall derive a value for the angle ϕ in our parametric construction from the velocities of the components of the emission lines. We shall show that the angle ϕ is relatively insensitive to assumptions made regarding the systemic velocity and the expansion velocity of the individual blobs, that is, ϕ appears to be relatively well determined even when there are significant uncertainties in the interpretation of the velocity data. Further, we shall estimate the blob expansion velocity $w = dr/dt$ in several ways to arrive at a value which is probably uncertain by roughly a factor of 2. This will turn out to be sufficient accuracy for the analysis to proceed.

The observed, heliocentric velocities of the four major components of Hβ for four representative dates are shown in Figure 3. Before we can find the angle ϕ from the observed velocities we must first subtract from each component the systemic velocity v_s and also the effects, if any, of the blob expansion velocity $w = da/dt$. Whether or not the expansion of the blobs contributes to the apparent velocities of the individual components depends on the actual geometry and the transfer of radiation through the individual condensations. It is therefore not clear that subtracting the mean of all the components from each component will give the best results. In particular we expect some differences between the pairs of blobs in a more realistic model; also, the mean velocities of the pairs $a + d$ and $b + c$ are not the same (Table 2) and do not vary in the same way with time (Fig. 3). For the velocities tabulated in Table 2 and for the purpose of finding ϕ, we have chosen to take the average of each pair, $a + d$ and $b + c$, as approximately equal to $(v_s - w)$ appropriate for that pair. The resulting velocities are listed in Table 2, as are the angles ϕ derived from setting $v_b/v_a = v_c/v_d = \tan \phi$.

In Figure 3, on the other hand, we have sketched the average of all four components as a function of time. Using these values as $(v_s - w)$ would give values of ϕ between 20° and 30°, averaging around 24° as for the other approach but showing more scatter. Both because it is physically more reasonable and because it shows less scatter in the resulting values of ϕ, we feel that the pair-wise average is more sound.

The angle ϕ appears in any case to be fairly well determined and reasonably constant, with a value equal to ~24°. We shall consider this the "most likely" value of ϕ; however, because of the uncertainty inherent in our assumptions that the pairs of blobs (*a*) have the same ejection velocity and (*b*) emerge at right angles, we shall continue to examine the consequences

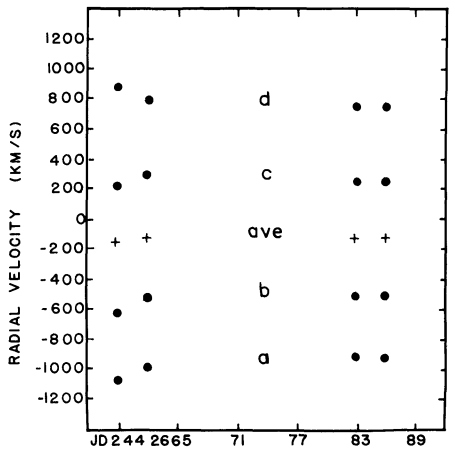

FIG. 3.—The observed heliocentric velocities of the components of Hβ as a function of time (*filled circles*) and also the mean velocity of all four components for each date (*crosses*).

TABLE 2

CENTER-OF-MASS VELOCITIES DERIVED FROM PAIRS OF COMPONENTS

DATE	VELOCITY RELATIVE TO CENTER OF MASS		$V_{system} - w$		
	a, d[a]	b, c[a]	a, d[a]	b, c[a]	$\phi \equiv \arctan(v_{b,c}/v_{a,d})$
Sept. 3 (JD 2,442,659)	955	420	−75	−220	24°
Sept. 6 (JD 2,442,662)	890	405	−90	−115	24°
Sept. 28 (JD 2,442,684) Oct. 1 (JD 2,442,687)	825	385	−95	−135	25°
Mean	...	...	−87	−157	24°

[a] Components used.

of other choices of ϕ in evaluating our other parameters.

Finally, we need to estimate the expansion velocity of the individual blobs, $w = da/dt$. The simplest method is to use the widths of the individual components and assume that it is entirely due to the expansion of the blobs; that approach yields $w \approx 100$ km s^{-1}. This value is entirely consistent with the velocities shown in Figure 3 and Table 2: the mean values of $v_s - w$ were -135 to -150 km s^{-1} for most of the observations, which corresponds for example to a system velocity of ~ -50 km s^{-1} with an expansion velocity of ~ 100 km s^{-1}. For the analysis which follows we shall assume $w \approx 100$ km s^{-1} within a factor of 2; this will provide sufficient accuracy for the analysis based on our simple, approximate model.

b) *Derivation of* $K \sin j$, q_1, *and* q_2

To illustrate the procedure used in determining $K \sin j$, q_1, and q_2, the analysis of the intensities of the components of Hβ for September 3 (JD 2,442,659) to September 18 (JD 2,442,674) is shown in Figure 4). On September 3 the intensities of components a and b were the same, indicating $(K \sin j) = 0$; on that date, however, components c and d were considerably weaker, indicating that at least q_1 and possibly also q_2 were not zero. On September 14, on the other hand, $K \sin j$ is large, q_1 is zero, and q_2 is nonzero. On September 18 and subsequent dates the points show increased deviation from the line drawn for a single $K \sin j$; this is probably due to contamination of the line profile by blends.

The values of the anisotropy constant ($K \sin j$) and the occultation parameters (q_1, q_2) derived from the line ratios for Hα, Hβ, Hγ, and Hδ are shown in Figure 5. Hα and Hδ are probably severely affected by blending after September 6, causing the derived $K \sin j$ to behave in an irregular fashion. From the behavior of all four lines before September 6 and from the behavior of Hγ and Hβ for all the times shown, the following

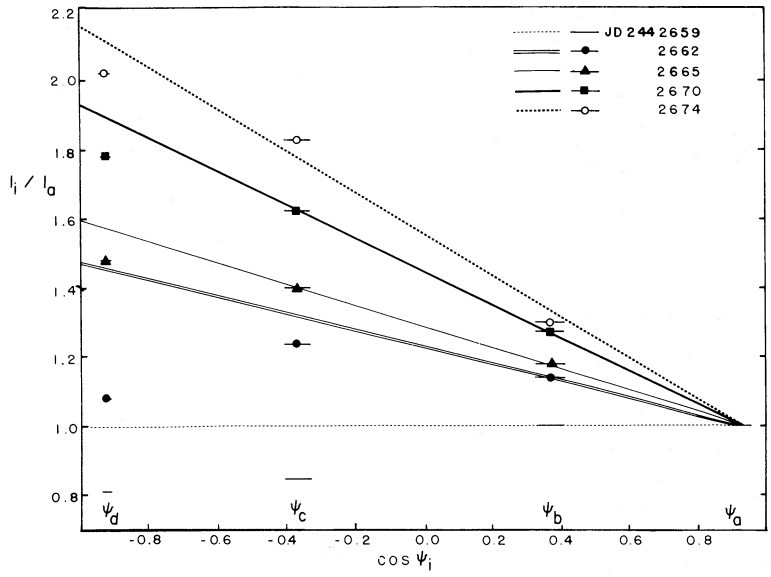

FIG. 4.—Relative intensities of the components of Hβ plotted as a function of Ψ for several dates. Straight line fits for $K \sin j$ values fitting I_b/I_a are also shown. For the earliest dates, occultation reduces the intensity of the redshifted components (c and d) so that the positions of I_c/I_a and I_d/I_a fall below the values predicted by eq. (3).

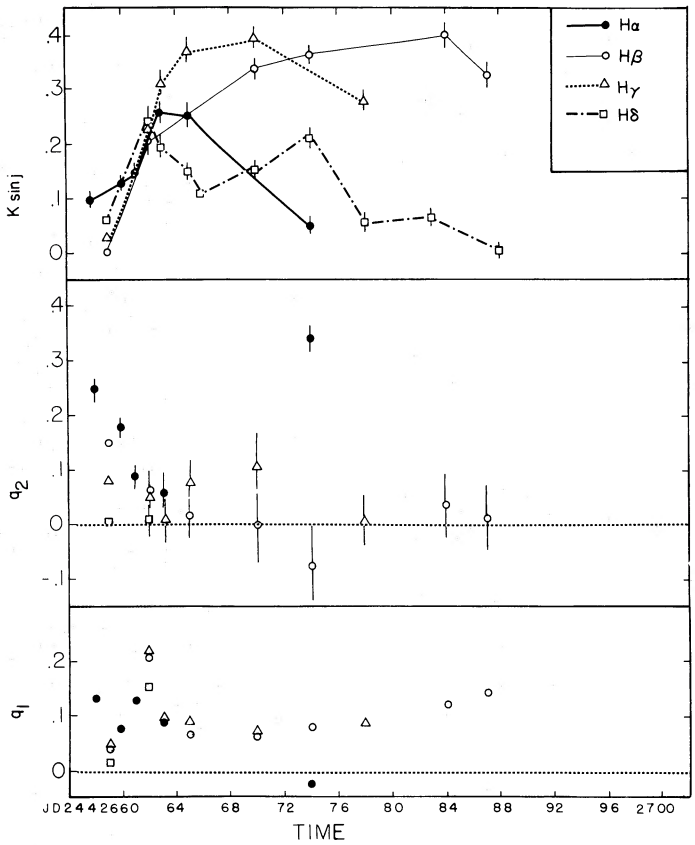

FIG. 5.—Derived parameters $K \sin j$, q_1, and q_2 as a function of time for the four hydrogen Balmer lines. $K \sin i$ values for Hδ after September 6 (JD 2,442,662) are anomalously low because of blending of the line; q_1 has not been calculated for those dates for Hδ. Note that q_2 remains positive well after q_1 becomes 0, indicating that a model with an equatorial ring is likely to provide a better interpretation than four distinct blobs. Error bars for $K \sin j$ and q_2 indicate the range of solutions obtained by varying ϕ from 20–30°.

three important qualitative conclusions may be drawn:

1. The anisotropy factor K increases rapidly to a maximum of $\sim(0.4/\sin j)$, then gradually decreases ($\sin j$, of course, is assumed to remain constant).

2. Occultation effects ($q_1, q_2 \neq 0$) are present during the first week; after September 9 occultation effects are probably not significant.

3. On September 3 the occultation parameter q_1 is different for each of the lines, with $q_1(\mathrm{H}\alpha) > q_1(\mathrm{H}\beta) > q_1(\mathrm{H}\gamma) > q_1(\mathrm{H}\delta)$; this is exactly what we would expect to find if the "occultation" is in fact due to partial absorption of the components with $\tau_{\mathrm{H}\alpha} > \tau_{\mathrm{H}\beta} > \tau_{\mathrm{H}\gamma} > \tau_{\mathrm{H}\delta}$. Differential reddening (as found by Hutchings and Fisher (1973) for FH Ser could also be partially responsible for this effect, however.

Our three conclusions regarding $K \sin j$, q_1, and q_2 each have important implications for the evolution of the nova system.

As mentioned above, the remaining differences between the intensity ratios and the resulting parameters for the different hydrogen lines and, in particular, the behavior of Hδ after September 6 (JD 2,442,662) and probably also of Hγ after September 22 (JD 2,442,678) can be ascribed to the blending of other lines with the hydrogen profiles. We have chosen for this reason to emphasize parameters derived for Hβ, which appears from Figures 2 and 5 to be least contaminated by blends of the lines considered.

The most interesting result in the present analysis is conclusion (1), the behavior of the anisotropy parameter K. We find K to be relatively insensitive to our choices of ϕ. Thus, its increase from zero to $\sim 40\%$ and its subsequent decrease appear to be real effects. This behavior is unlikely to be highly dependent on geometry the way ϕ and q_2 (and to a lesser extent q_1) are. Also, the behavior of K is consistent with several reasonable physical models for the evolution of the blobs; one of these is discussed in some detail in § V.

The duration of the occultation effect (conclusion [2]) is a simple consequence of $w \ll v$. If we assume $w \sim 100$ km s^{-1}, $v \gtrsim 1000$ km s^{-1}, and $R_0 \approx r_0 \approx 6$ AU on September 3 (see § IV*c*), then $R/r \gtrsim 1.3$ on September 6 and $R/r \gtrsim 1.6$ by September 9, when q_1 and q_2 indicate that occultation is no longer important.

In § IV*c* we shall derive geometric parameters $\sin j$ and R/r for September 3 from the values of q_1 and q_2 found for Hβ; conclusion (3) suggests that these

parameters will not be as simply related to the actual geometry of the nova as some of the other parameters are. We shall proceed with the analysis despite this uncertainty, however, simply in order to show that the values of the angles which result are quite consistent with those values for the inclination of the equatorial plane, sin i, for example, found by a number of other investigators using different geometric models, if a reasonable identification of sin i with angles from our model is made, and therefore that sin i is probably reasonably model independent.

The behavior of the parameter q_2 shown in Figure 5 is quite irregular, including negative values as well as positive ones. We conclude that q_2 is probably neither a meaningful nor a well-determined parameter. This is expected; as we commented earlier, q_2 depends on the determination of both q_1 and K and is thus very sensitive to errors in the data or the analysis. Further, if one considers the model of Hutchings (1972) generally considered to be the most likely to apply, then the system consists of one pair of polar blobs plus one ring of material. When such a system is "forced" into a scheme with four identical components, as we have done, one expects the blocking of the farthest component to be the first parameter to break down, since partial absorption by ring material is very unlike blocking by overlapping opaque spheres.

c) *Occultation Effects and Geometric Parameters for September 3*

In this section we shall show how a simple geometric blocking scheme can be used to derive R/r and sin j for the early stages of development of the ejecta. As was discussed in § IV*b*, it is not clear that the simple geometrical interpretation really applies to the actual nova. The purpose of this portion of the analysis is, then, just to show that such an approach gives parameters which are in reasonable agreement with equivalent parameters found by other investigators for other models and, hence, that these parameters are probably reasonably model-independent.

For this section we shall assume that our four identical blobs are opaque spheres of radius r. To determine the fraction of each blob's light which is blocked by another blob, we will need to find the apparent separation of the centers of a pair of blobs compared to the blob radius r:

$$\delta_{ij} = \frac{\text{apparent separation of } i, j}{2r} . \tag{6}$$

We will relate this parameter to the occultation parameters q_{ij} by assuming

$$q_{ij} \approx \frac{\text{area blocked}}{\pi r^2} . \tag{7}$$

This involves a further approximation: we are now ignoring the previously assumed anisotropy in this calculation of the effect of the blocking. That is, for purposes of calculating the amount of light lost as a result of occultation, we ignore the dependence of the radiation of the blobs on the angle. This assumption, which vastly simplifies the calculations, is not expected to introduce any more uncertainties than have already been introduced by (*a*) the assumptions of identical, spherical blobs and (*b*) the assumption of completely opaque blobs. As long as $K \sin j$ is not too large (and we found it always to be $\lesssim 0.4$ in § IV*a*), then the errors introduced by using equation (7) will be no larger than the errors expected to be introduced by other assumptions we have already made. A simple calculation of a "worst possible case" will illustrate this: assume $j = 90°$ and that the blocked region has uniform intensity $I = I_0(1 + K)$, while the region which is visible has $I = I_0(1 - K)$. Then the apparent occultation parameter derived from the observations using our assumption of uniform blobs, $q_{\rm app}$, will be related to the "true" blocking parameter, q, by

$$q_{\rm app} = \frac{1 + K}{1 - K} q . \tag{8}$$

Since the maximum value of $K \sin j$ observed was 0.4, then we must have $q \lesssim q_{\rm app} \lesssim 2q$. Since in practice j is not 90° (we will find $\sin j \approx 0.6$) and since we also made extreme assumptions regarding the intensity distribution in deriving equation (8), in practice we expect that $q \lesssim q_{\rm app} < 1.5q$. This implies a maximum expected error of roughly 50% from the use of uniform intensity in this derivation of the geometry. Note once again that the largest uncertainty in the analysis occurs in the attempt to find specific geometric parameters using a particular model for the blocking. The analyses presented in all the other sections of this paper are subject to much less uncertainty since (*a*) the results are less sensitive to the assumptions made and (*b*) fewer assumptions need to be made.

A straightforward geometric derivation relates the blocking parameter q to the apparent separation of the pair of blobs by:

$$q = \left[\frac{2}{\pi} \arccos \delta - \delta(1 - \delta^2)^{1/2}\right] . \tag{9}$$

This expression is readily inverted to find δ using a tabulation of δ versus q, assuming $q = 0$ when $\delta \geq 1$.

The final step is to relate the apparent separation to the geometric parameters R/r and sin j. Writing

$$\delta_{ij} = \frac{(y_i - y_j)^2 + (z_i - z_j)^2}{4r^2} , \tag{10}$$

and using the coordinates from equation (1) we find expressions for $\delta_1 = \delta_{ac} = \delta_{bd}$ and $\delta_2 = \delta_{ad}$:

$$\delta_1 = \frac{R}{2r}(1 + \cos^2 j - 2 \sin \phi \cos \phi \sin^2 j)^{1/2} , \tag{11}$$

and

$$\delta_2 = \frac{R}{r}(1 - \cos^2 \phi \sin^2 j)^{1/2} . \tag{12}$$

Given δ_1 and δ_2 (from "observed" q_1 and q_2) and ϕ (from the velocities), we can, in principle, solve equations (11) and (12) for the two unknowns R/r and $\sin j$. If either q_1 or q_2 is zero, however, we can only use these relations to solve for the minimum R/r (as a function of $\sin j$) which is consistent with the lack of blocking.

For the observations used in this paper, there is really only one date which definitely satisfies q_1 and $q_2 > 0$, that is, September 3, with $q_1 = 0.15 \Rightarrow \delta_1 = 0.74$ and $q_2 = 0.04 \Rightarrow \delta_2 = 0.90$. For that date we have calculated R/r and $\sin j$ for a range of assumed ϕ; the results are listed in Table 3.

From the parameters ϕ and j listed in Table 3 and the velocities $w = 100$ km s^{-1}, $v \approx 1000$ km s^{-1}, we can determine from equation (11) the date at which δ_1 should equal 1 (and hence $q_1 = 0$). From equation (11) we find $R/r = 1.44$ will suffice for the blocking parameter q_1 to equal zero; from the velocities and the assumption that $R_0 = r_0 \approx 6$ AU on September 3 (JD 2,442,659), we find that q_1 should vanish between September 6 and September 9. From the values of q_1 in Figure 5 it is clear that q_1 does in fact become negligible between September 6 and September 9.

Note that the R/r values found in Table 3 are ~ 1.07 to 1.11, while four disjoint spheres cannot be any closer together in the arrangement of Figure 2 than $R/r = \sqrt{2}$. We derive this apparently contradictory result as a consequence of two of our assumptions: (1) that the blobs are completely opaque (so a relatively small area of overlap produces sufficient blocking) and (2) that we are dealing with identical spherical blobs. We have already discussed some of the limitations of these two assumptions in §§ I and II.

The reason for pursuing this analysis, despite its obvious shortcomings, is to provide a means of comparing our model with those of other investigators and notably the ring/blob models of Hutchings (1972; see also Soderblom 1976). In particular we seek to answer two questions: Is the Hutchings model "forced" on us by the observed line behavior, or will other quite different models be likely to satisfy observational constraints equally well? How well determined are such parameters as the inclination of the system to the plane of the sky from the observational constraints? Our conclusions will be that the ways in which our model fails to account for observed properties of the nova do indeed suggest a model along the lines of the Hutchings model and also that parameters such as the inclination of the system are remarkably well determined from the observations and do not depend heavily on the assumptions going into the models.

TABLE 3

GEOMETRICAL PARAMETERS FOR SEPTEMBER 3[a]

$\tan\phi$	R/r	$\sin j$	j	Ψ_a	v
0.25	1.11	0.64	40°	52°	1450
0.30	1.10	0.63	39°	53°	1500
0.35	1.09	0.61	38°	55°	1550
0.40	1.08	0.60	37°	57°	1610
0.45	1.07	0.59	36°	58°	1670

[a] The outward velocity of the blob is $v = v_{\rm outer}/\cos\Psi$; $\Psi_a = \cos^{-1}(\cos\phi \sin j)$ is the angle between the line of sight and $\boldsymbol{R}_a$.

In Table 3 we have tabulated two angles: j, the inclination of the system plane with respect to the line of sight, and Ψ_a, the angle between the line of sight and the line from the system center to the closest condensation, blob a. In order to compare the angles we have found with those of other investigators, we must first derive a correspondence between our four-blob model and their equatorial ring-polar blob model. We have already argued that the limb-brightening of the ring will mimic a second pair of blobs. In order for the occultation to be in the sense that is observed, i.e., in order for the component with maximum redshift to be the one subject to maximum occultation, then we are further forced to identify blob a as a polar blob, and hence our angle Ψ_a is the same as the angle i in Hutchings's (1972) model. Hutchings and McCall (1977) found that an angle of inclination of the ring of $\sim 60°$ was required to enable the equatorial ring/polar blob model to correctly reproduce the emission line profiles. Hutchings, Bernard, and Margetish (1978) found $i \approx 50°$ from a further study of the line profiles including an analysis of the 3 hr profile modulations. All of the values of Ψ_a listed in Table 3 fall in the range 52–58°, in complete agreement with the values found from the equatorial ring/polar blob analyses. Thus it seems likely that the angle of inclination is a fairly model-independent quantity and, hence, that it will be ~ 50–$60°$ for all reasonable models of Nova Cygni 1975.

What evidence can this analysis provide regarding the validity and necessity of the Hutchings model? We have shown that at least one of its quantitative predictions, the inclination of the system to the line of sight, is relatively model independent. In § V we shall show that the mass of the ejecta and the amount of ionizing flux required are, to within an order of magnitude, also model independent. We shall now argue that the failures of our model to consistently model all of the observations strongly suggest that the Hutchings model is in fact the correct type of model for this nova.

The evidence supporting the Hutchings model derived from our analysis can be very briefly stated:

1. Throughout the period covered by the observations q_2 remains positive. This suggests that q_2 is caused by occultation of the far polar component by a ring of material, so that as the system expands the blocking persists.

2. An attempt to fit the occultation geometry for September 3 yields $R/r \approx 1.1$, whereas disjoint spheres must have $R/r \geq \sqrt{2}$. The wedge-shaped ring and blobs of the Hutchings model are not so restricted.

3. Since, $q_1(\mathrm{H}\alpha) > q_1(\mathrm{H}\beta) > q_1(\mathrm{H}\gamma) > q_1(\mathrm{H}\delta)$, this suggests that transfer effects in partially opaque condensations are required.

Thus, two essential features of the Hutchings model—the presence of an equatorial ring and the roughly wedge-shaped geometry of that ring—are suggested by the specific failures of the simpler, well-determined, four-blob model.

V. THE EVOLUTION OF INDIVIDUAL CONDENSATIONS AND THE PHYSICAL INTERPRETATION OF K

In this section we shall first describe two simple "spot" models which could be used to explain the anisotropy of the radiation emerging from the blobs. We then discuss in considerable detail the implications of interpreting the anisotropy as due to partial ionization of the blobs. Based on a simple "Strömgren crescent" geometry for the ionization we will be able to derive information on the ionization state, electron density, and total mass of the ejecta plus conditions on the source of the ionizing radiation. These numbers will then be found to be consistent with results found by other investigators from independent arguments. Based on this agreement we can finally conclude that the partial ionization interpretation is likely to be correct and hence that the key ingredient for the interpretation of the evolution of the hydrogen emission line profiles in this nova is the ionization balance in the ejecta.

a) Spot Models

To produce anisotropic radiation from a spherical blob which is close to a source of radiation one can invoke several mechanisms. The simplest mechanism is an opaque blob with a "hot spot" on the side facing the source of radiation. Here there are several parameters describing the hot spot (source function relative to the back-side area of the spot) and the evolution with time is quite arbitrary. Although this is clearly a possible model, it has too many free parameters to be well determined from the data, and we will consider other more well-defined models in more detail.

A variation on the simple spot mechanism is a "dark spot" model which assumes that for a region on the side away from the source the temperature (or source function) is so low that radiation from that spot is negligible; this leaves only one parameter for the model, the area of the cold spot. It is simple, then, to relate the parameter K to the area of the cold spot:

$$\frac{1-K}{1+K} = \frac{\pi r^2 - \text{apparent spot area}}{\pi r^2} = 1 - \left(\frac{\rho}{r}\right)^2, \tag{13}$$

where $\rho = r \sin\theta$ is the radius of the spot. For the maximum $K \sin j$ observed, 0.4, using $\sin j = 0.6$ (from Table 3) gives $K_{\max} = 0.66$ and hence $\sin\theta = \rho/r < 0.89$. Alternatively, if we merely divide the blob into two uniform hemispheres and let the source function as S_1 on the "hot hemisphere" and S_2 on the cool one, we find $S_2/S_1 = (1-K)/(1+K) = 0.4/\sin j = 0.66$, or a 60–80% reduction in the source function will suffice. We conclude that spot models—both hot-spot and cold-spot models—can be made to fit the variation of K with reasonable parameter values.

b) The Partial Ionization Model

The most physically interesting possibility is that the blob is partially ionized, with a sharp boundary between neutral and ionized zones, as in a Strömgren sphere. Assume that the ionized volume radiates the observed emission lines and is transparent to them and that the unionized volume is opaque to these lines. Such a model is schematically presented in Figure 6. The neutral region will be all points $\geq \Delta x$ distant from the irradiated side; the maximum ionized volume visible, giving maximum intensity, is

$$V_{\max} = \frac{4\pi r^3}{3}\left[\frac{3}{2}\left(\frac{\Delta x}{2r}\right) - \frac{1}{2}\left(\frac{\Delta x}{2r}\right)^3\right], \tag{14}$$

and the minimum

$$V_{\min} = \frac{4\pi r^3}{3}\left(\frac{\Delta x}{2r}\right)^3. \tag{15}$$

Thus

$$\frac{1-K}{1+K} = \frac{2(\Delta x/2r)^2}{3-(\Delta x/2r)^2}. \tag{16}$$

Note that the maximum K observed, ~ 0.66, corresponds to $\Delta x \approx r$ or to roughly 30% of the blob's material in the neutral zone.

This model for the anisotropy has the appropriate temporal evolution as well. If we assume an ionization equilibrium is maintained (since recombination time $\ll R/v$), then we can write directly

$$S_{\mathrm{UV}}(W) = \alpha N_e^2 [4\pi r^3 (f)/3], \tag{17}$$

where $S_{\mathrm{UV}}(W)$ is the flux of ultraviolet photons from the central source incident on the blob (W is a dilution factor, $W \doteq r^2/4R^2$), and f is the fraction of the blob

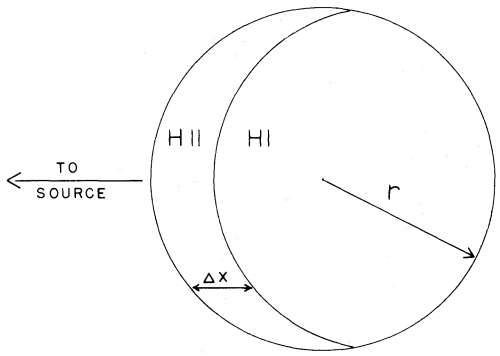

FIG. 6.—Schematic "Strömgren crescent" model corresponding to a partially ionized spherical blob. The thickness Δx of the ionized region is assumed to be constant as measured parallel to the line connecting the center of the sphere to the source of the UV radiation.

which is ionized. Rearranging and using $N_e \propto r^{-3}$ we find

$$f = \frac{K_{\rm UV}}{N_e(0)^2 r_0^6}\frac{r^5}{R^2} = \frac{K_{UV}}{N_e(0)^2 r_0^6}\frac{(r_0 + wt)^5}{(r_0 + vt)^2}, \quad (18)$$

where $K_{\rm UV} = S_{\rm UV}/(16/3\pi\alpha)$ is assumed not to vary, and $N_e(0)$ is the electron density at $t = 0$. If we now assume $dr/dt \ll dR/dt$ and $r \approx R_0$ at $t = 0$ (corresponding roughly to September 3), it is clear that f will first decrease as a result of the $1/R^2$ term (decrease in stellar UV), then increase as a result of the exponent in r^5 (decreased density effect).

In Figure 7 we show a sample theoretical fit to K as a function of time using equations (15), (17), and (18) for Hβ and assuming $\sin j = 0.66$. We find for Hβ (which is the least affected by blends) that velocities $v \gtrsim 1000$ km s^{-1} and $w \lesssim 100$ km s^{-1} fit very well for $w/r_0 = 0.015$ per day and $v/r_0 = 0.1$ per day, i.e.,

$$r_0/w \approx (6\ \text{AU})/(150\ \text{km s}^{-1})$$

and

$$r_0/v \approx (6\ \text{AU})/(1000\ \text{km s}^{-1}). \quad (19)$$

Thus we find for Hβ that velocity parameters chosen from an analysis of the displacements and widths of the line components, yield an almost perfect fit for the anisotropy parameter as a function of time (based on the simple partial ionization model for the anisotropy of the radiation field) with $r_0 = R_0 = 6$ AU on September 3. We have not attempted to fit $K(t)$ for the other lines, since blending is apparent in the profiles and that renders $K(t)$ more uncertain for those lines. Note that although the outburst occurred on August 29–30 (Hutchings, Bernard, and Margetish 1978) the blobs do not emerge as separate on our scheme until nearly a week later.

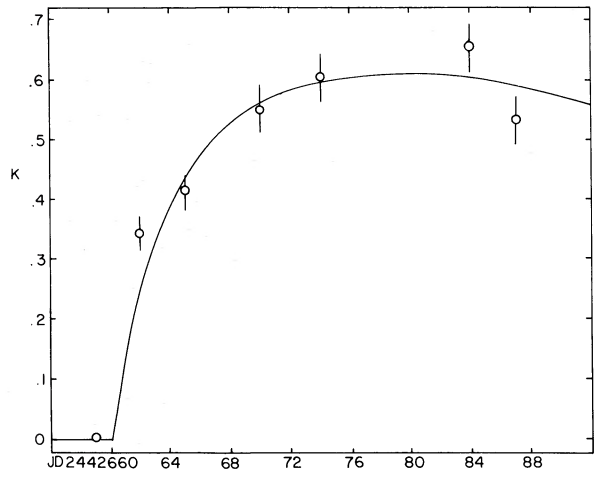

FIG. 7.—Theoretical fit to $K(t)$ for Hβ from eqs. (16) and (18) with $\sin j = 0.6$, using $r_0/w = (3\ \text{AU}/100\ \text{km s}^{-1})$, $r_0/v = (3\ \text{AU}/1000\ \text{km s}^{-1})$, and $t = 0$ on August 31.

For comparison with the dimensions derived here consider the analysis by Campbell (1976) of short-term variations in Hα. He found (for a spherical model) the radius of the ionized region to be ~ 7 AU at maximum, August 31, and 12–15 AU on September 5. With the approximations required for both his estimates and ours, and the differences in assumed geometry, this is quite good agreement.

Our model of partially ionized blobs suggests an explanation for another feature of novae, namely the breaking up of the major components into several smaller ones as the nova evolves. In a partially ionized blob the radiation pressure will tend to be concentrated on the far, neutral, high-opacity spot and, hence, will accelerate it slightly away from the rest of the blob (Haas 1977). The breakup of the large blob into smaller ones should be expected to continue until the decrease in density leads to a completely ionized system at the beginning of the nebular phase; then it will cease. This is consistent with the conclusions of Gallagher and Anderson (1976) that the basic velocity structure in HR Del was established by the beginning of the nebular stage and has not changed substantially in a period of approximately 6 years since the early observations of Sanyal (1974).

The other parameter needed in fitting $K(t)$ is the coefficient $K_{\rm UV}/[N_e^2(0)r_0^3]$; we find this to be

$$K_{\rm UV}[N_e^2(0)r_0^3] \approx 2, \quad (20)$$

which may be rearranged to give

$$S_{\rm UV} \approx 8 \times 10^{47}[N_e(0)/10^9]^2(r_0/6\ \text{AU})^3\ \text{photons s}^{-1}. \quad (21)$$

Since $N_e(0)$ found by other investigators is $\sim 10^9$ (see especially Ferland and Shields 1978; and also Neff *et al.* 1978 for N_e as a function of time) and since $r_0 \approx 6$ AU (§ IV*c*) we find $S_{\rm UV} \approx 10^{47}$ to 10^{48} photons s^{-1}. This is consistent with, for example, the flux expected from a white dwarf of radius $\sim 0.01 R_0$ and $T \approx 350$–$400{,}000$ K; it is also in agreement with the results of Ferland (1977) that $S_{\rm UV} = 2.6 \times 10^{47}$ photons s^{-1}.

From our dimension r_0 for September 3 we can also estimate the total mass of the ejecta: assuming total ionization ($N_e = N_{\rm H}$) we have

$$M \approx x(4/3)\pi r_0^3 N_e(0) m_{\rm H}$$
$$\approx 10^{28}\ \text{g} \times (x/2)[N_e(0)/10^9](r_0/6\ \text{AU})^3, \quad (22)$$

where x is a geometric factor which takes into account the fact that $r_0 = R_0$ is not possible for distinct spheres. For reasonable geometries we typically find $1 \lesssim x \lesssim 4$. This gives an order-of-magnitude estimate for the total mass ejection of $\lesssim 4.10^{-5}\ M_\odot$ in the form of blobs, with total kinetic energy $\sim 10^{44}$ ergs.

Summarizing this section: we have used a simple partial ionization model to (1) successfully reproduce

$K(t)$ and (2) find $S_{UV} \approx 10^{47}$–10^{48} photons s^{-1} for the central ultraviolet source, and for the ejecta $M \approx 4 \times 10^{-5}\ M_{\odot}$ and total K.E. $\approx 10^{44}$ ergs. These order-of-magnitude results are in complete agreement with the results of other investigators.

VI. SUMMARY

We have shown that a very simple four-blob scheme with anisotropically radiative spherical blobs is able to explain the relative intensities of the major components of the hydrogen lines, primarily as a result of an evolving "anisotropy parameter" K. Consideration of physical explanations for the behavior of the anisotropy parameter led us to suggest a partial ionization model which explains nicely the breakup of the blobs into smaller components; the partial ionization model also gives estimates for the total ultraviolet photon flux from the ionizing source on the order of 10^{47}–10^{48} photons s^{-1} and of the total mass of the ejecta on the order of 10^{28} g. This model plus the velocity data suggest also that on September 3 the blobs were together (separation distance between blob centers approximately equal to blob diameter) and that the region had a diameter of ~ 12 AU.

By analyzing carefully the behavior of the parameters as a function of time, the different behavior of the parameters for different lines, and the places where the model fails to self-consistently explain the observations, we have been able to suggest some essential features of any more realistic model: more realistic models must include (*a*) an equatorial ring or equivalent extended region, (*b*) radiative transfer effects in the hydrogen lines, and (*c*) the effects of anisotropic radiation fields caused by partial ionization of the ejected condensations during the early decline phase.

Finally, we would like to reiterate that this scheme works remarkably well considering its simplicity, and hence our results suggest that future work in modeling the development of line profiles in novae should consider the variation of physical conditions within the regions of condensations responsible for the emission line components. This may well be more informative than pursuing ever more complicated geometries. The agreement of our results with those of other investigators using different models also indicates that several geometric parameters are quite model independent; in particular R/r, v and w, r_0, and sin i do not seem sensitive to the exact geometry assumed.

It is a pleasure to thank the staff of the Dominion Astrophysical Observatory who made some of the observations reported here. Thanks are also due to Dr. R. H. Koch for helpful discussions and to J. S. Gallagher, John Hutchings, and G. Bowen for comments on earlier drafts. A. Sanyal would like to thank the director of DAO for the facilities extended to him during his stay there in the summer of 1975. This research was partially supported by NSF grant AST 76-18036.

REFERENCES

Campbell, B. 1976, *Ap. J.* (*Letters*), **207**, L41.
Ennis, D., Becklin, E. E., Beckwith, S., Elias, J., Gatley, I., Matthews, G., Neugebauer, G., and Willner, S. P. 1977, *Ap. J.*, **214**, 478.
Ferland, G. J. 1977, *Ap. J.* (*Letters*), **212**, L21.
Ferland, G. J., Lambert, D. L., and Woodman, J. H. 1977, *Ap. J.*, **213**, 132.
Ferland, G. J., and Shields, G. A. 1978, *Ap. J.*, **226**, 172.
Gallagher, J. S., and Anderson, C. M. 1976, *Ap. J.*, **204**, 625.
Gallagher, J. S., and Ney, E. P. 1976, *Ap. J.* (*Letters*), **204**, L35.
Haas, M. 1977, Ph.D. thesis, Iowa State University.
Hutchings, J. B. 1972, *M.N.R.A.S.*, **158**, 177.
Hutchings, J. B., Bernard, J. E., and Margetish, L. 1978, *Ap. J.*, **224**, 299.
Hutchings, J. B., Bernard, J. E., Margetish, L., and McCall, M. 1978, *Pub. Dom. Ap. Obs. Victoria*, **15**, 73.
Hutchings, J. B., and Fisher, W. F. 1973, *Pub. A.S.P.*, **85**, 122.
Hutchings, J. B., and McCall, M. L. 1977, *Ap. J.*, **217**, 775.
Jenkins, E. B., *et al.* 1977, *Ap. J.*, **212**, 198.
Neff, J. S., Smith, V. V., and Ketelsen, D. A. 1978, *Ap. J. Suppl.*, **38**, 89.
Sanyal, A. 1974, *Ap. J. Suppl.*, **28**, 115.
———. 1976, *Pub. A.S.P.*, **88**, 741.
Soderblom, D. 1976, *Pub. A.S.P.*, **88**, 517.
Strittmatter, P. A., *et al.* 1977, *Ap. J.*, **216**, 23.

A. Sanyal: Department of Physics and Astronomy, Howard University, Washington, DC 20059
L. A. Willson: Erwin W. Fick Observatory, Physics Department, Iowa State University, Ames, IA 50011